JOURNAL OF GEOPHYSICAL RESEARCH, VOL. 100, NO. A11, PAGES 21,343–21,355, NOVEMBER 1, 1995

Strongly enhanced incoherent-scatter plasma lines in aurora

Sheila Kirkwood and Hans Nilsson
Swedish Institute of Space Physics, Kiruna, Sweden

Jean Lilensten and Marina Galand
Centre d'Etudes des Phénomènes Aléatoires et Géophysiques-ENSIEG, St. Martin d'Heres Cedex, France

Abstract. Observations of incoherent-scatter plasma-line intensities, measured in the *E*-region with the European Incoherent Scatter UHF radar, during auroral precipitation , are presented. Intensities up to 200 times the thermal level were observed in a restricted frequency interval from 5.5 to 6.5 MHz. Intensities were lower at both higher and lower frequencies. The intensities are compared with quantitative estimates based on model suprathermal electron fluxes for the prevailing conditions. The minimum in suprathermal electron fluxes between 2 and 4 eV, which is caused by the excitation of vibrational levels in N_2 , is found to result in a minimum in expected plasma-line damping and a maximum in intensity between 5.5 and 6.5 MHz, for the EISCAT UHF wavelength. Good agreement is found between the calculated and observed intensities.

Introduction

Incoherent-scatter plasma lines are a somewhat neglected tool for studying the electron component of the ionospheric plasma. Incoherent-scatter radars usually make use of the ion-line, the signal scattered from ion-acoustic waves in the plasma. Analysis of the spectrum of the scattered signals gives information on thermal plasma density, plasma temperatures, and ion drifts under various assumptions of radar calibration, ion-mass and particle energy distribution. Plasma lines represent signals scattered from Langmuir waves in the plasma and are sensitive to the density, energy distribution and motion of the electron component of the plasma. In principle, their observation offers the possibility to measure electron drifts, to determine electron density and temperature independently of the assumptions necessary in the ion-line case and to obtain information on the distribution of suprathermal electrons. The former parameters influence the frequency at which the plasma lines are observed, the latter determine their intensity, so both properties must be measured to gain maximum information.

In practice, there are a number of experimental and theoretical problems in the measurement of plasma lines. The intensity of the signals is often too weak to allow them to be detected, so that they must be enhanced by photoelectrons or aurorally generated suprathermal electrons to be observable. They appear at a frequency offset from that transmitted by about the plasma frequency, i.e., a few MHz. This varies rapidly both with altitude and with time (particularly in aurora) and makes it difficult, first to "catch" the signal, and then to measure the frequency accurately with limited altitude or time resolution. Most of the quantitative studies which have been published so far have made use of the more stable and predictable plasma lines which are observed during quiet daytime conditions. For example, *Kofman et al.* [1981], *Fredriksen et al.* [1989], and *Kirkwood and Bjørnå* [1992] have demonstrated their application for daytime temperature measurements. *Yngvesson and Perkins* [1968], *Cicerone* [1974], *Kofman and Lejeune* [1980], and *Bjørnå and Kirkwood* [1986] have shown how they can be used to study photo electron fluxes. In the case of electron drift measurements it has been found that the theoretical basis for the interpretation of the difference in offset frequencies between up- and down-shifted plasma lines is as yet inadequate [*Kofman et al.*, 1993; *Mishin and Hagfors*, 1994; *Nilsson et al.*, 1995].

The number of studies of plasma lines during aurora is limited. *Wickwar* [1978], *Kofman and Wickwar* [1980] and *Oran et al* . [1981] present and discuss observations made using the Chatanika (Alaska) incoherent scatter radar. Plasma lines were monitored with 8 to 20 min time resolution and appeared between 98- and 134-km altitudes. Intensities were 0.06 to 1.2 eV, i.e., enhanced 3-60 times above the thermal level (see the section below on plasma line intensities for an explanation of these terms). These enhancements and their variation with altitude were found to be consistent with those expected from model calculations of the suprathermal electron flux. The absence of plasma lines below 98 km could be explained by collisional damping of the plasma line. *Kofman and*

Paper number 95JA00765.
0148-0227/95/95JA-00765$05.00

Wickwar [1980] also compared the difference in offset frequencies between up- and down-shifted plasma lines just above the *E* region peak. They found an average 10-kHz difference during a 30-min period of diffuse aurora, which they interpreted as a downward field-aligned current of about 10 $\mu A\ m^{-2}$ carried by the thermal electrons. However, their uncertainties were large and 10 $\mu\ Am^{-2}$ is substantially higher than would be expected in such circumstances. The question of the ability of plasma lines to give measurements of field-aligned currents in aurora is still an open one.

Valladares et al. [1988] reported more comprehensive observations of aurorally enhanced plasma lines from the same radar, now relocated to Søndre Strømfjord (Greenland). The time resolution was now improved to 30 s, and both up- and down-shifted plasma lines were monitored in alternating 30 s intervals. Plasma lines were observed between 160 and 190 km (they would have been at higher frequencies than could be monitored at lower heights) and intensities found to be as high as 9 eV, i.e. up to 150 times the thermal level. These high intensities were suggested to be due to some plasma instability. Some differences were observed between the intensities of up- and down-shifted lines, but these were considered to be insignificant, given that they were not measured exactly simultaneously. Valladares et al. also attempted to determine electron temperatures by comparing the offset frequency of the plasma lines with the plasma frequency determined from the ion-line measurements. The results were consistent with the ion-line estimates of electron temperatures, but the scatter was very large, of the order of 500 K.

In a recent theoretical paper, *Mishin and Schlegel* [1994] have discussed the strong enhancements observed by Valladares et al. and proposed that they cannot be explained as an enhancement by the suprathermal electrons. They propose, rather, that they are enhanced by plasma turbulence, accompanied by extremely high electron temperatures, which is supposed to occur in a thin layer during auroral precipitation. However, the data published by Valladares et al. were insufficient to test this hypothesis completely.

Here we present a more comprehensive set of observations of plasma lines during aurora than has previously been published. We present truly simultaneous observations of both up- and down-shifted plasma lines, with better time resolution (10 s), better frequency coverage, and higher plasma line intensities than previous reported measurements. We show that these measurements can be applied to determining electron temperatures, and in some circumstances electron drifts, with high time resolution during auroral precipitation. We further demonstrate that the high plasma line intensities can be explained by a reasonable suprathermal electron flux and that they are not consistent with the plasma-turbulence model.

Measurement Technique

The experiments reported here were made with the European Incoherent Scatter (EISCAT) UHF radar, situated near Tromsø in northern Scandinavia. Three radar pulses were transmitted 5-12 ms apart, one 60 μs , one 360 μs and one 1200 μs long at 930, 929.5, and 931 MHz, respectively. The last pulse was received only at the remote receiving sites in Sodankylä and Kiruna. At the transmitting site, two receiving channels were tuned to the frequencies of the two shorter pulses, and the received ion-line signals processed to give a power profile at 3-km altitude intervals (for *E* region electron density) and autocorrelation functions at 30.5-km altitude intervals for *F* region densities, temperatures, and ion drifts. Plasma lines from both pulses were monitored using the filter-bank technique, i.e., six of the radars' eight receiving channels were tuned to appropriate frequencies offset upward and downward from those transmitted by between 4.5 and 6.9 MHz. At any one time, the plasma-line offsets monitored were $+x$, $-x$, $+(x+0.2)$, $-(x+0.2)$, $+(x+0.4)$, $-(x+0.4)$, $-(x+0.5)$, $-(x+0.7)$, $-(x+0.9)$, $+(x-0.5)$, $+(x-0.3)$, $+(x-0.1)$ MHz, where x was 5 or 6 MHz (in each channel the band covered was +-25 kHz, controlled by the final receiver filters). Thus the frequency interval covered at any time was 1.4 MHz with 0.1- to 0.2-MHz resolution and simultaneous monitoring of both up- and down-shifted plasma lines at three frequencies. The basic time resolution of the measurements was 10 s.

The antenna was, for technical reasons, directed vertically during these experiments, which means about 13° north of parallel with the magnetic field. The altitudes covered were from ~80 to ~600 km. Measurements were made on the evenings of August 3, 6 ,7 and 10, 1990. No plasma lines were observed on August 3 or 7, which were quiet with no significant auroral activity. On August 10 there was some weak auroral precipitation and strong plasma lines were observed in the *F* region, but not in the *E* region On August 6, however, strong, intermittent auroral precipitation was observed by the radar from 1750 UT until observations ended at 2100 UT. A substorm onset was indicated by the magnetometer at about 2030 UT. Plasma lines were detected at and near the *F* region peak during most of the interval 1750-2100 UT, but these are not the subject of this study. Plasma lines in the *E* region were detected for only a few minutes in association with the appearance of intense auroral precipitation in the radar beam, at ~1800, 1825, 1940, and 2030 UT, which we refer to as events a, b, c and d, respectively. The electron density fluctuations associated with these activations, the associated plasma-line intensities, and the derived electron temperatures are shown in Plate 1. The derivation of the electron temperature and the plasma line intensity are described in the relevant sections below. The "electron density" shown in Plate 1 is, to be more exact, the raw electron density, n_e', where

$$n_e' = n_e\left(\frac{2}{(1+K^2D^2)(1+K^2D^2+T_e/T_i)}\right) \qquad (1)$$

where n_e is the true electron density, T_e the electron temperature, T_i the ion temperature, K the scattering-wave vector, and D the Debye length ($D^2 = \varepsilon_0 kT_e/n_e e^2$, k is Boltzmanns constant, and e is the electron charge).

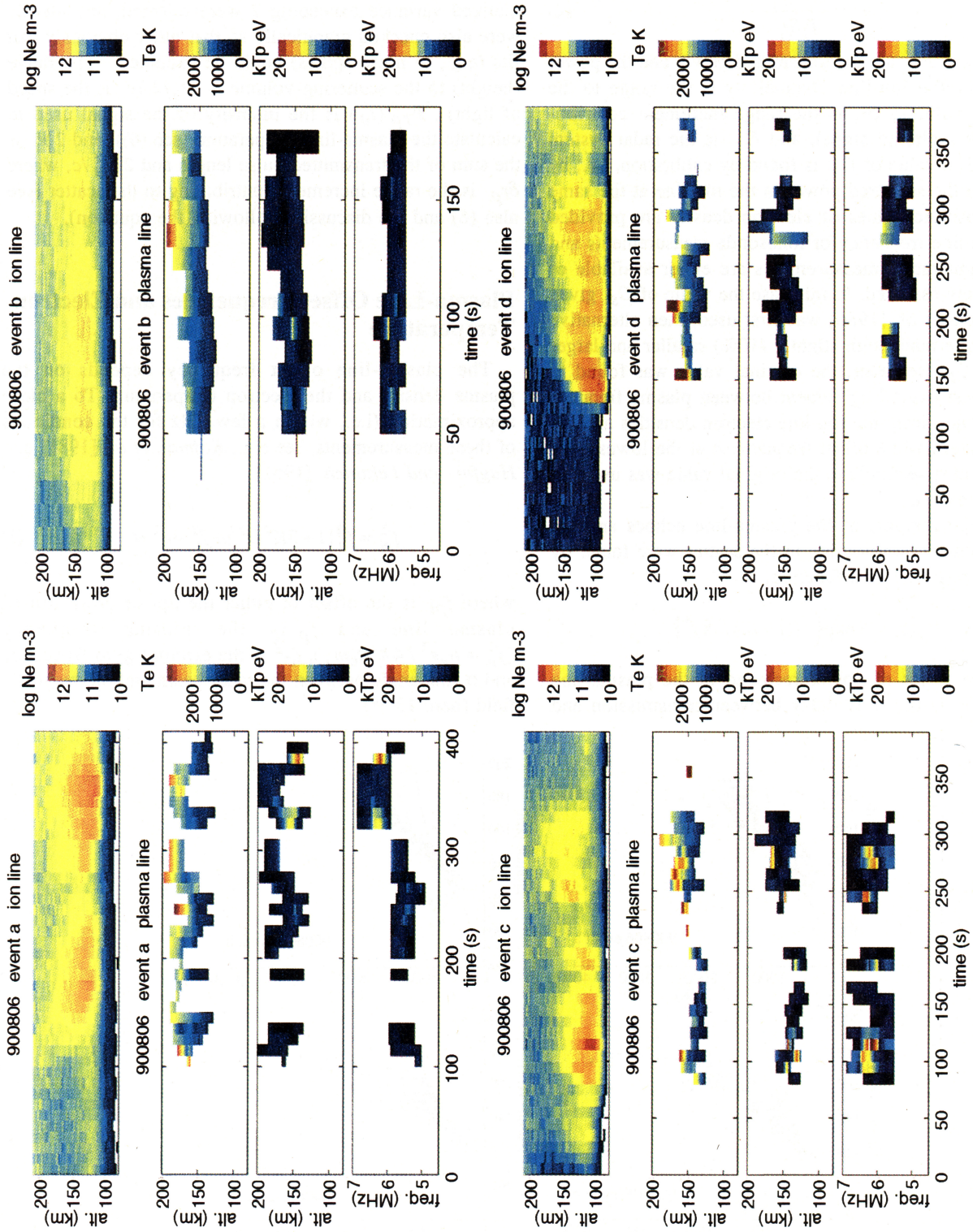

Plate 1. Raw electron densities (N_e), electron temperatures (T_e) and plasma line intensities (kT_p) for four events on August 6, 1990: event a, 1755.10-1802.00 UT; event b, 1822.10-1825.20 UT; event c, 1935.50-1942.20 UT; and event d, 2028.50-2035.20 UT. See text for details.

In the ionospheric E region where T_e and T_i are low and close to equal, $n_e' \approx n_e$. The raw electron density is calculated from the power received in the ion-line part of the incoherent scatter spectrum:

$$n_e' = \frac{C_s P_{ri} r_i^2}{P_t \delta r_i} \tag{2}$$

where P_t and P_{ri} are the transmitted power and the power received in the ion-line channel, r_i is the range to the scattering volume, δr_i is the range increment contributing to the scattered signal, and C_s is the radar system constant. The value of C_s is found by calibration, i.e., by monitoring the scattered power in the ion line at the same time as absolute values of electron density are provided by plasma-line frequency or ionosonde measurements and plasma temperature measurements are either available or can be safely assumed. In this case the value of C_s given by *Kirkwood et al.* [1986] was first used, then alternative analysis were made with slightly (10%) smaller and larger values of C_s. However, the original value was found to give the best overall agreement between plasma frequencies calculated from the ion-line electron densities and the observed plasma-line offset frequencies at the lowest altitudes (see next section), so the original value was used for the final analysis.

The range (height) of the plasma-line echoes and the range increment contributing to the scatter were found by least squares fitting of a function,

$$P_{rp}(t) = S \exp\left\{-((t-t_0)/\delta t)^6\right\}$$

to the time series of power recieved in the plasma-line channels (t is the time delay between transmission and reception, P_{rp} is the power received in the plasma line channel, S, t_0 and δt are fitted parameters). This is a steep-sided, flat-topped function which can easily be fitted by standard computer procedures and gives a good fit to the shape of the received signal. All fits with a normalized variance exceeding 2 were rejected, and all fits were also checked graphically so that other obviously bad fits (e.g., to noise spikes) could be excluded. The range (height) to the scattering volume is $ct_0/2$ (c is the speed of light) , $P_{rp}(t_0)$ is the intensity of the signal used to calculate the plasma-line temperature (see (6)), and $2\delta t$ is the sum of the transmitted pulse length and $2\delta r_p / c$, where δr_p is the range increment contributing to the scatter (see also (6) and the discussion following the equation).

Plasma-Line Offset Frequencies and Electron Temperature

The plasma-line offset frequency depends on the plasma density and the electron temperature. To a close approximation (i.e., within a few kHz for the conditions of these measurements, see e.g., *Kofman et al.* [1981] and *Hagfors and Lehtinen* [1981]

$$f_{pl}^2 = f_p^2\left(1+3K^2D^2\right)+f_c^2 \sin^2\alpha \tag{3}$$

where f_{pl} is the offset of either the up- or down-shifted plasma line and f_p is the plasma frequency ($f_p^2 = n_e e^2 / 4\pi^2 \varepsilon_0 m_e$), f_c^2 is the electron gyro frequency and α the angle between the radar beam and the magnetic field (here 13.5°).

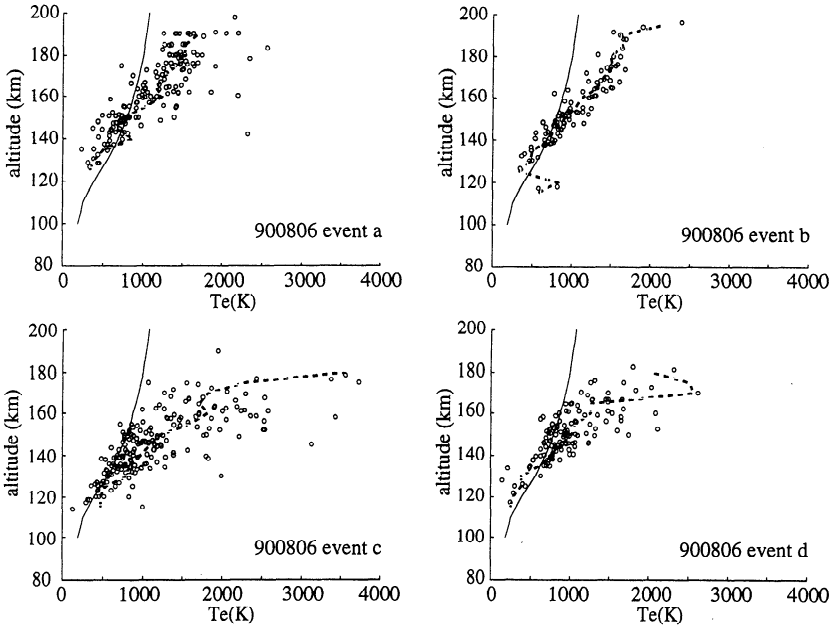

Figure 1. Circles show electron temperatures derived from the plasma-line offset frequency and ion-line power for each of events a-d. The solid line indicates the model of ion temperature (assumed equal to MSISE-90 neutral temperature [*Hedin*, 1991]), which was used in the calculation. The dashed line indicates the mean of the derived temperatures in each 5-km altitude bin.

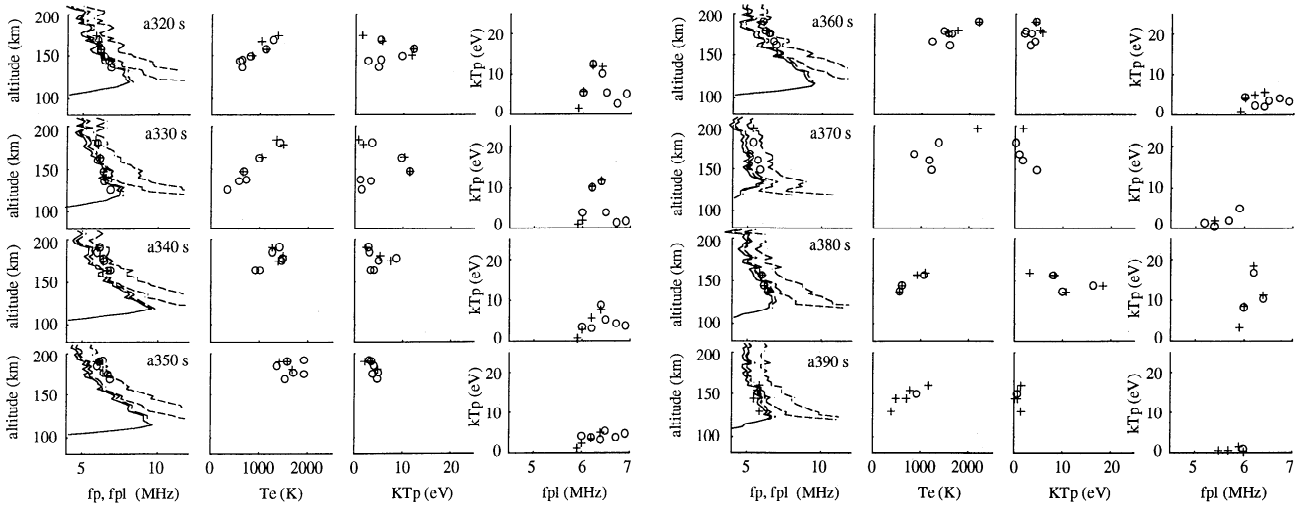

Figure 2. Individual profiles for a number of 10-s integration intervals from event a. The times shown above each set of profiles correspond to the times shown on the x axis in Plate 1. The leftmost altitude profile shows "raw" plasma frequency calculated from the ion-line power (solid line), the expected offset frequency for plasma lines for three different assumptions of electron temperature, $T_e = T_i$, T_e = 1000 K, and T_e = 2000 K (dashed lines, highest T_e corresponds to dashed line furthest from the solid line), and the measured offset frequencies of the plasma lines (circles and crosses). The altitude profiles second from the left show electron temperatures derived form the plasma-line frequency and ion-line power. Altitude profiles second from the right show the plasma-line intensity . The rightmost diagrams show the plasma-line intensity as a function of offset frequency. In all diagrams, up-shifted (crosses) and downshifted (circles) plasma lines are indicated separately.

The electron temperature can be found from

$$T_e = \left(\frac{f_{pl}^2}{f_p^2} - \frac{f_c^2 \sin^2 \alpha}{f_p^2} - 1\right) \cdot \left(\frac{n_e e^2}{3K^2 \varepsilon_0 k}\right) \qquad (4)$$

We do not know n_e at the outset, only n_e' (see (1)), so that the solution must be obtained by iteration and assuming model values for T_i. Electron temperatures estimated using (4) are shown in Plate 1 and Figures 1, 2, and 3. The first observation, in Figure 1, is that they are close to the model T_i at the lowest altitudes, as expected. This is a good indication that the value of C_s used in calculating n_e' is correct. Increasing (or decreasing) C_s by 20% gives a corresponding increase (or decrease) in n_e' and f_p^2. This results in a systematic decrease (or increase) of the derived T_e by about 100 K at T_e = 500 K, increasing to 400 K at T_e = 2000 K. The agreement between the derived T_e and the model at the lowest altitudes, and between the lowest T_e and the model at higher

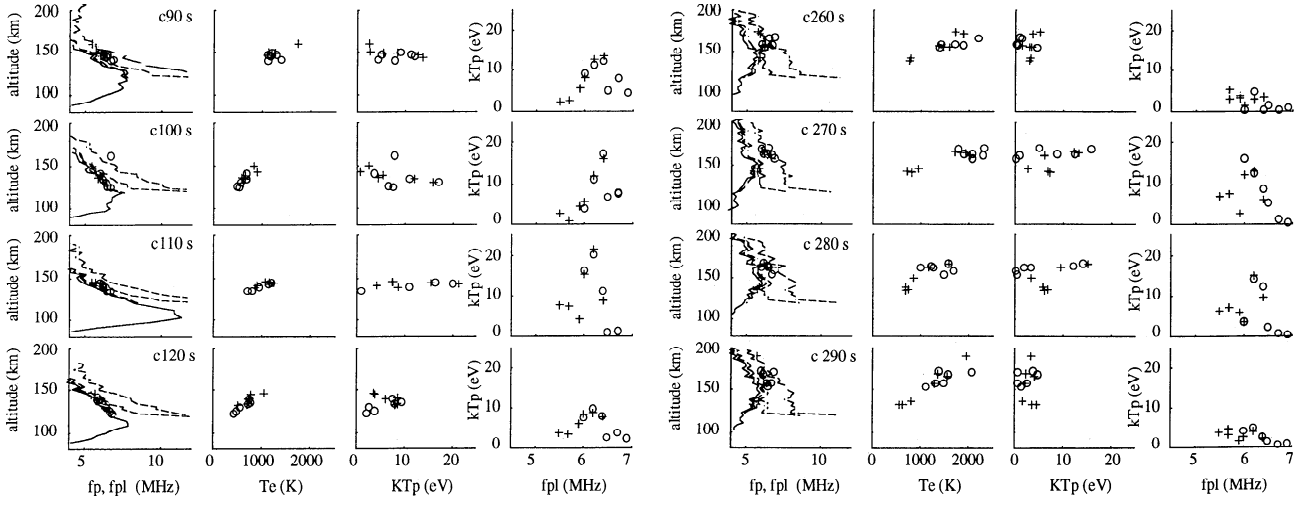

Figure 3. As for Figure 2, but profiles are from event c.

altitudes, indicates that the accuracy of C_s is within 20%. The possibility of a systematic error of a few hundred degrees Kelvin at the higher altitudes is in many cases not significant considering the scatter, but should be borne in mind when interpreting the results.

In event b, where the plasma density varied rather slowly, the temperatures show a well-defined altitude profile, increasing from about 1000 K at 150-km altitude to 2000 K at 190-km altitude (Figure 1, event b). This is similar to temperature profiles measured during aurora using the incoherent-scatter ion lines [e.g., *Lilensten et al.*, 1990]. For the other events, and particularly event c, the temperatures appear more variable and reach higher values, up to 3000 K at heights as low as 160 km (Plate 1 and Figures, events a, c, d). The precipitation in these cases is also more intense, so higher electron temperatures might be expected. However, plasma densities also vary on time scales comparable to the integration time of the measurements which can lead to erroneously high (or low) electron temperatures, i.e., if the average plasma density during the integration interval is less (more) than the plasma density at the time the plasma-line scatter is produced. Since plasma-line intensifications seem to be related to precipitation, it is more likely that the electron temperatures will be overestimates than underestimates, but clearly they should be interpreted with some caution when the plasma density is changing rapidly.

However, there is one interval of distinctly enhanced temperature, not associated with rapidly changing electron densities, in event c (c250 s - c300 s, where we use the shorthand "c250s" to mean event c, time 250 s). In this interval temperatures exceed 2000 K at altitudes as low as 150-160 km (Plate 1, event c, and Figure 3). This appears to be a real temperature increase. It is supported by the observations at several plasma-line frequencies, for four 10-s integrations in a row, and appears to be associated with softer particle precipitation than at other times. It is, however, possible that the radar is looking through an aurora (the beam is directed vertically, not along the field line) so that the precipitation on the field line where the high temperatures are observed may have different characteristics from that indicated by the electron density profile at lower altitudes.

Plasma-Line Offset Frequencies and Electron Drift

In principle, a drift of the thermal electron population should result in a Doppler shift of the plasma lines, so that the offsets of the up- and down-shifted lines from the transmitter frequency are unequal. In practice, the slightly different wave vectors at the frequencies of the up- and down-shifted lines also lead to asymmetry [e.g., *Kofman et al.*, 1993]. If we can measure the asymmetry, and correct for the latter effects, we can measure the electron drifts. In the present measurements a difference in offset frequency between the up- and down-shifted plasma lines will appear as a different altitude for the corresponding returns in the fixed-frequency monitoring channels. To first order, the asymmetry is given by

$$f_+ - f_- = (h_+ - h_-)df/dh \quad (5)$$

where $h+$ and $h-$ are the altitudes of the up- and down-shifted plasma lines and df/dh is the gradient in the plasma-line frequency (estimated by a suitable fit to measurements from a number of heights, see below). In practice, we can determine the altitudes to better than 1 km but df/dh can be very large, varying from about 10 kHz / km in event b to 200 kHz / km during the most intense precipitation in event c. As a result, the errors in determining the plasma-line asymmetry can vary between a few kHz and several tens of kHz. This is clearly seen in the results, which are shown in Figure 4. Note, first, that the frequency scale for the panel showing event b is a factor of 10 less than for the other events. We might expect electron drifts of the order of a few tens to a few hundred of m s^{-1}, corresponding to an asymmetry of a few hundred Hz to a few kHz. The additional asymmetry due to the different wave vectors should contribute similar amounts, a few hundred Hz for temperatures around 200 K, 10 times as much for 2000 K. Only in event b do we get good enough accuracy for the measurements to be useful, and in this case there is no evidence for any significant asymmetry. It seems that this method will not be useful for electron drift measurements in the conditions when such measurements are of most interest, i.e. when there is intense energetic particle precipitation, at least not in the E region, where the plasma density gradients are large.

Plasma-Line Intensities and the Suprathermal Electron Flux

Observations

A convenient way of expressing the plasma-line intensity is given by the plasma-line "temperature" kT_p,

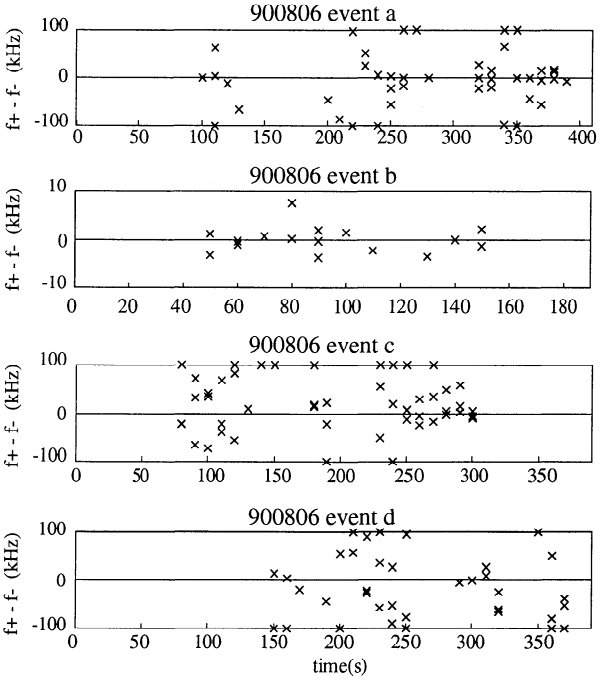

Figure 4. The difference between the offset frequencies of the up- and down-shifted plasma lines ($f+ - f-$) for each event. See text for details.

which is simply the temperature of the purely Maxwellian plasma which would give the same plasma-line intensity. The observed plasma-line temperature is calculated from the incoherent-scatter measurements of the power scattered from the plasma using the expression (derived from equations (1) and (2) above and *Yngvesson and Perkins* [1968, equations 16 and 17] transformed to SI units)

$$kT_p = \frac{A_{pl} C_s P_{r_p} r_p^2}{P_t \delta r_p} \quad (6)$$

where P_t is the transmitted power, P_{rp} is the power received in the plasma-line channel, r is the range to the scattering volume, δr_p is the range increment contributing to the scattered plasm-line signal, C_s is the radar system constant as described above and $A_{pl} = g^+ e^2 / \varepsilon_0 K^2$, where g is a gain factor found by calibration (using observations of radio stars) to account for different gains in the radar system at the frequency of the ion-line echo, where C_s is measured, and at the frequencies of the up- and down-shifted plasma lines. In this case, $g+ = 0.95$ and $g- = 1.16$, for the frequency range of up- and down-shifted lines, respectively.

The term in the expression (6) for kT_p which is most difficult to estimate is δr_p, the range increment contributing to the scatter. It depends on the gradient of the plasma-line offset frequency with range (height) , df_{pl}/dr , and the width of the receiver filter, BW. In principle, this can be estimated in three ways, and all three methods were tested in the present analysis. The first method is simply to measure the length of time, Δt, during which the signal is received. Then $\delta r_p = c(\Delta t - \tau)/2$, where c is the speed of light and τ is the length of the transmitted pulse. In practice, the range increment contributing to the scatter is often much less than the range resolution available in these experiments, so that this method gives a large scatter in the results, with apparently less-than-zero range increments at times. The second possibility is to estimate df_{pl}/dr from the electron density profiles and multiply by BW. In this case, we have only the raw electron density profile readily available. The true electron density decreases less rapidly with altitude than the raw electron density, so that df_{pl}/dr estimated from the raw electron density is systematically too high and the resultant δr_p too small. This could be improved using a model of the temperature increase with altitude, but in the present case this seems to be unnecessary, as the third method gives good results. The third possibility is to estimate df_{pl}/dr from the measured f_{pl}. Since we generally see plasma lines at a number of frequencies (and altitudes) at any one time we can estimate df_{pl}/dr by fitting a suitable polynomial to the observations. In this analysis we have fitted a quadratic, which gives a good fit in all cases and allows us to estimate δr_p whenever we observe plasma lines at at least four frequencies simultaneously (up- or down-shifted as they are fitted together).

An overview of the observed plasma-line intensities is given by Plate 1. It can be seen that plasma lines are observed almost all of the time when there is precipitation (indicated by enhanced electron densities) and that kT_p is usually less than 10 eV. However, on a number of occasions kT_p exceeds 10 eV, at times reaching 20 eV. This usually occurs only in a limited height /frequency interval, with lower kT_p at both higher and lower heights/frequencies. There is no obvious correlation between the occurrence of these strong plasma-line enhancements and the intensity of the precipitation, but the varying altitude coverage would make such an effect hard to discern. Close examination of the lower two panels for each event in Plate 1 shows that the enhancements occur at altitudes from 130 to 170 km (e.g., event c) but only over a restricted frequency interval, 5.7-6.4 MHz. This is shown more clearly by Figure 5. Figures 2 and 3 show the strongly enhanced plasma lines and associated plasma density and temperature profiles in more detail for two occasions: the time interval 320-390 s from event a, and 90-120 s and 260-290 s from event c. In these figures the leftmost column shows a series of profiles, each representing a 10 s integration, comparing the plasma frequency and plasma-line offset frequency calculated from the power in the ion line with the measured offset frequencies

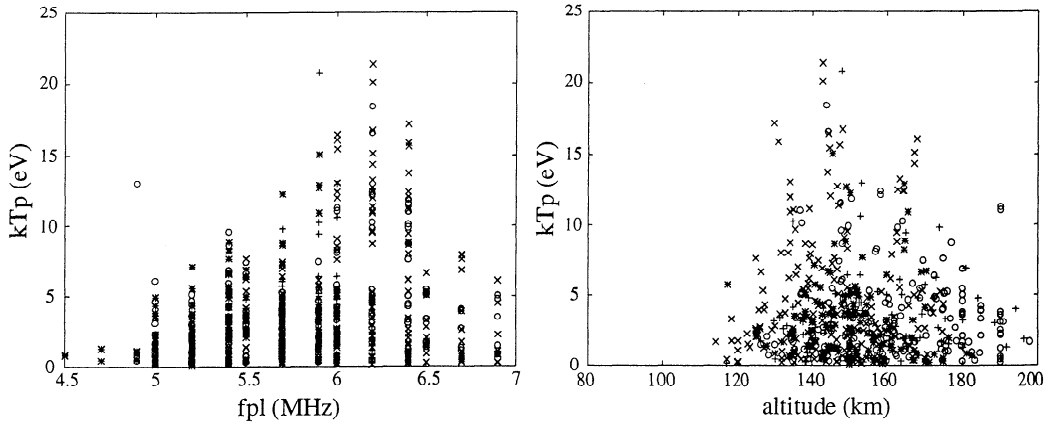

Figure 5. Observations of plasma-line intensity for all four events plotted as a function of altitude (right panel) and offset frequency (left panel). Event a, (circles), event b, (plus signs), event c, (crosses) and event d, (stars).

of the plasma lines. The solid line shows the "raw plasma frequency," ($f_p' = \left(n_e e^2 / 4\pi^2 \varepsilon_0 m_e\right)^{1/2}$), which would be the same as the plasma-line offset frequency in a cold plasma. The three profiles indicated by the dashed lines in Figures 2 and 3 show the expected plasma-line offset frequencies for $T_e = T_i$ (model), T_e = 1000 K, and T_e = 2000 K, at progressively increasing offsets from f_p'. The circles show the measured offsets for the up-shifted plasma lines, the crosses for the down-shifted lines. In all cases, the observed plasma line offsets are consistent with those expected from the ion-line analysis, with electron temperatures between the model values (a few hundred degrees Kelvin) and 2000 K. In all the cases shown in Figures 2 and 3, the profile of f_p' decreases steadily with altitude above the peak (apart from some noise), as expected for an ionization profile caused by auroral precipitation. In a few cases not shown in Figure 3 or 4 but visible in Plate 1 (c130s, c140s), there appears to be a narrow layer of enhanced electron density superimposed on the normal topside gradient. Since the radar beam was not directed parallel to the magnetic field, this is probably caused by the beam intersecting two spatially distinct auroral arcs. Even in these cases, the plasma-line offset frequencies are in good agreement with those expected from the ion-line analysis and temperatures close to or less than 2000 K.

Last of all we consider the plasma-line intensities, shown in the two rightmost columns in Figures 2 and 3. In event a, Figure 2, the maximum plasma-line intensity is initially about 12 eV, exceeding 5 eV throughout a ~20 km thick layer centered at ~160 km altitude and covering a frequency interval 6-6.5 MHz. Ten seconds later, the thickness of the layer has increased to 40 km, but the frequency interval involved remains the same. In the subsequent 30 s the electron densities increase and the height from which the plasma line signals we are monitoring are returned increases to above 170 km. This is accompanied by a decrease in plasma line intensities to about 4 eV for all frequencies. In the last 30 s shown (a370s-a390s), electron densities fall and we again see plasma lines from lower altitudes, 130-160 km. For the middle 10 of these last 30 s, strongly enhanced plasma-lines ~20 eV are seen at ~145 km altitude, again for 6.0 to 6.4 MHz frequencies. The plasma-lines in this frequency interval come from lower altitudes, and appear to correspond to substantially lower electron temperatures at 380 s compared with 370 s, which may explain the increased intensity (see below). In the last 10 s (a390s) the plasma frequency seems to have fallen too low to give plasma lines above 6 MHz.

Figure 3 shows the most intense plasma lines which were observed during these experiments, exceeding 20 eV in one 10 s integration (c110s) and persistently exceeding 10 eV for as long as 40 s (c90s-c120s). The altitude of the intensity maximum varies from 130 km to 150 km with the width of the layer of enhancement in this case being only 10 km or less. In terms of frequency, the enhancement above 10 eV is again confined to the interval 6-6.4 MHz, but intensities in the interval 5.5-6.0 MHz reach almost 10 eV. The strongest plasma lines during this event correlate with the strongest precipitation (c110s). On the other hand, there are periods with apparently very different levels of precipitation, c100s and c270s, but with very similar plasma-line intensities. The second part of Figure 3 shows the results from 260 s to 290 s. Here the precipitation seems to be relatively weak (the electron densities are rather low), but electron temperatures, and at times plasma-line intensities, are high. It is possible that the radar is looking through a narrow arc in this case, so that the precipitation on the field line where the plasma-lines are seen is more intense than appears to be the case.

Although we have not discussed this above, Figures 2 and 3 show the plasma line intensities for up- and down-shifted lines separately, and it can be seen that those intensities are close to equal. Figure 6 shows a comparison of up- and down-shifted plasma line intensities for all the observations, which confirms this. Thus, to explain our observations, we need a mechanism which strongly enhances plasma lines in a limited frequency interval from 5.5 to 6.4 MHz, over a rather wide altitude range, 130-170 km, and enhances both up- and down-shifted plasma lines equally.

Interpretation: Enhancement by Suprathermal Electrons

We first test the possibility that the plasma lines may be enhanced by suprathermal electrons. The intensity of the plasma lines is then determined by the energy input to the corresponding Langmuir waves, from thermal and suprathermal electrons, or from collisions, and by the damping of the waves by the same processes. The observation of equal intensities for down- and up-shifted plasma lines implies that the electron velocity distribution in the plasma for the energies affecting the plasma lines (a few eV) must be symmetric in the up-going and down-going directions, respectively. Since the eV population is formed by degradation and scattering of a

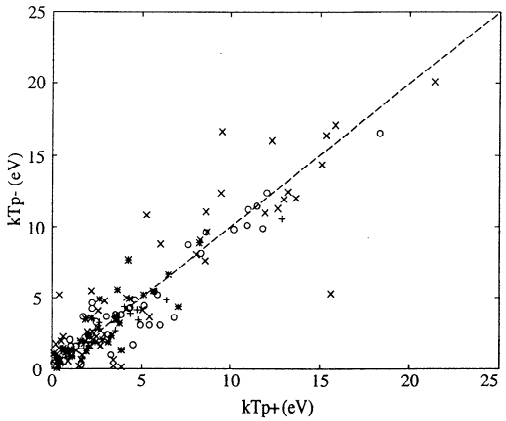

Figure 6. Comparison of the intensities of up-shifted (kT_{p+}) and down-shifted (kT_{p-}) plasma lines for event a, (circles), event b, (plus signs), event c, (crosses), and event d, (stars). The line indicates where $kT_{p+} = kT_{p-}$.

primary beam of down-going keV electrons, the velocity distribution at eV energies in intermediate directions is likely also to be the same as for the up and down directions, i.e., the plasma is isotropic at eV energies. Since an isotropic plasma is always stable against Langmuir wave instabilities, we can use the expression of *Yngvesson and Perkins* [1968] for the intensity of either the up- or down-shifted plasma line:

$$kT_p = \frac{kT_e\left(f_m(v_\phi)+f_s(v_\phi)+\chi\right)}{f_m(v_\phi)-kT_e\dfrac{d}{dE_\phi}f_s(v_\phi)+\chi} \tag{7}$$

where k is Boltzmann's constant, T_e the electron temperature, f_m and f_s the one-dimensional electron velocity distributions for the thermal (Maxwellian) and suprathermal populations, respectively, $v_\phi = \omega_{pl} / K$ is the electron velocity corresponding to the phase velocity of the Langmuir waves which scatter the radar signal, at frequency offset ω_{pl} and scattering wave vector K, E_ϕ the corresponding electron energy, and

$$\chi = \frac{n_e k_B T_e \nu_e}{m\pi K v_\phi^4}$$
$$\nu_e = \nu_{en} + \nu_{ei} \tag{8}$$
$$\nu_{en} = 5.4\times10^{-16} n_n (T_e)^{0.5}$$
$$\nu_{ei} = \left[34+4.18\log(T_e^3/(n_e\times10^{-6}))\right]\left[(n_e\times10^{-6})/T_e^{1.5}\right]$$

a collision term where n_n is the neutral number density, n_e the plasma number density, and m_e the electron mass [*Newman and Oran,* 1981; *Nicolet,* 1953]. The collisional term dominates the damping below 110 km [*Oran et al.,* 1981].

In the case of a purely Maxwellian plasma, in the absence of a magnetic field (or for waves propagating parallel to the magnetic field),

$$f(v_\phi) = n_e\left(\frac{m_e}{2\pi kT_e}\right)^{0.5}\exp(-m_e v_\phi^2/2kT) \tag{9}$$

and, in the absence of collisions, $kT_p = kT_e$.

In the case of propagation at an angle to the magnetic field, the effect can be accounted for by replacing the above Maxwellian expression for the thermal particles with [*Yngvesson and Perkins,* 1978]

$$f(v_\phi) = n_e\left(\frac{m_e}{2\pi kT_e}\right)^{0.5}\sum_{j=-\infty}^{\infty}\frac{\exp(-b\sin^2\theta)}{\cos\theta}I_j(b\sin^2\theta)\exp\left(\frac{-(y-j)^2}{2b\cos^2\theta}\right) \tag{10}$$

Where I_j is the modified Bessel function of the first kind, $b=K2kT_e/m_e\omega_C$, $y = \omega_{pl} / \omega$, ω_C is the electron cyclotron frequency, and θ is the angle between the scattering vector and the magnetic field.

For the suprathermal electrons, the one-dimensional velocity distribution must be found by numerical integration of the differential energy-flux spectrum. Figure 7 shows model calculations of the suprathermal energy-flux spectrum for the conditions corresponding to a320 s and c110 s in Figures 2 and 3. The corresponding one-dimensional velocity distributions $f_m(v_\phi)$, $f_s(v_\phi)$ for one of the cases are shown in Figure 8. The primary fluxes of energetic electrons (>3 keV) have been calculated by inverting the electron density profiles [*Kirkwood,* 1988; *Kirkwood and Eliasson,* 1990] and the resulting secondary fluxes have been calculated according to the procedure described in *Lummerzheim and Lilensten,* [1995]. As might be expected, the more energetic primary flux corresponding to c110s results in significantly higher secondary fluxes at low energies than in the case of a320s. The plasma-line intensities are most sensitive to the suprathermal electron distribution in the neighbor-

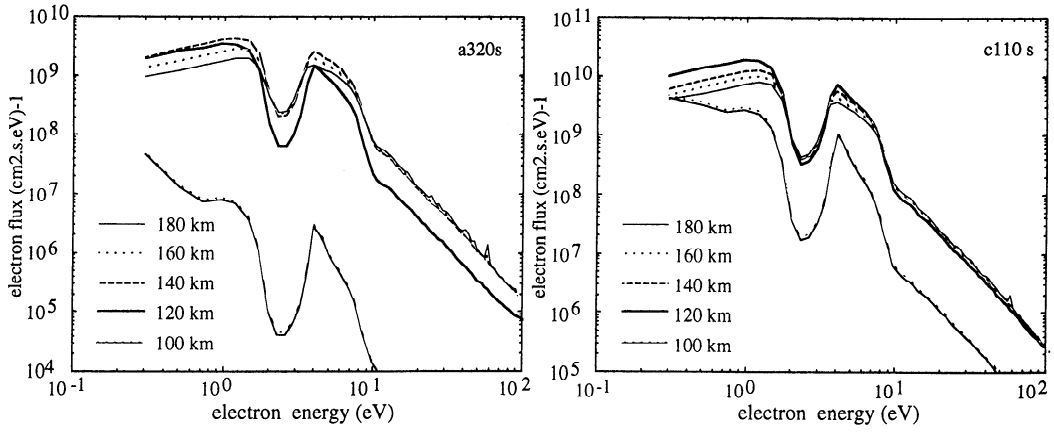

Figure 7. Model calculations of the flux-energy spectra of suprathermal electron spectra corresponding to the time labeled 320s in event a (a320s) and 110 s in event c (c110s). Only the upward flux is plotted but this is indistingushable from the downward flux in the energy range shown.

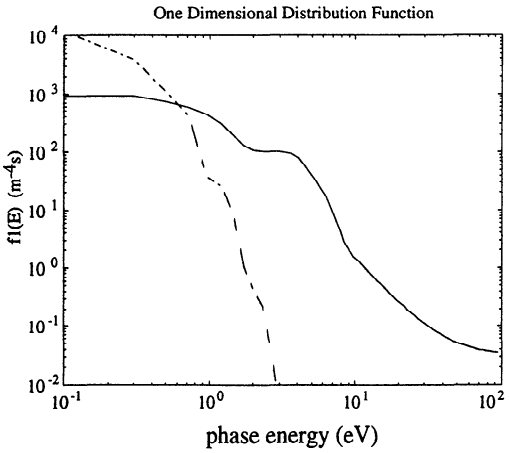

Figure 8. One-dimensional distribution functions $f_m(v_\phi)$ (dashed line), $f_s(v_\phi)$ (solid line) corresponding to the energy-flux spectrum for c110s, 120-km altitude in Figure 7.

hood of the phase-energy E_ϕ, which, for these observations corresponds to 1-4 eV. It is obvious from Figure 7 that the fluxes are strongly structured in this energy interval. This is due to excitation of the vibrational levels in N_2 and is a feature of the suprathermal electron distribution which is shown both by model calculations and in observations (by sounding rocket [*Sharp and Hays*, 1974]). Here it is worth noting that the dip in the suprathermal electron spectrum at 2-3 eV is most pronounced at the lowest height shown (100 km), where fluxes fall by a factor of 100 compared with the levels at 1 eV, and becomes progressively less pronounced as the altitude increases. The relative depth of the minimum is, on the other hand, rather constant for the different cases even though the overall flux levels are substantially higher in one case than the other.

Figure 9 shows the plasma-line intensities calculated using the suprathermal electron fluxes in Figure 7 and (7). Electron temperatures at the selected heights have been taken as the average from the profiles in Figure 1 and neutral densities from the MSISE-90 model (for $f_m(v_\phi)$, $f_s(v_\phi)$ and χ in (7). The values used are listed in Table 1. The curves in Figure 9 show a clear maximum in plasma-line intensities for frequencies corresponding to phase energies 2-3 eV, i.e. 5.5-6.5 MHz. The higher maximum intensities in event c compared to event a result from the higher levels of suprathermal electron flux in event c. The sharp decrease of intensities between 120 km and 100 km altitude is caused by a combination of decreasing suprathermal electron fluxes and an increase in collisional damping. The decrease in intensities between 160 km and 180 km altitudes is caused to some extent by the minimum in the suprathermal electron flux being less pronounced, but to a greater extent by increasing Landau damping by the thermal electrons as their temperature increases. This latter effect also pushes the maximum intensities to higher frequencies. Comparing with Figure 5, it can be seen that the intensity levels and overall form of the frequency dependence of the calculated plasma-line intensities are very similar to the measurements.

Figure 10 shows how the calculated intensities compare with the measured values for the times corresponding to, and adjacent to those used for calculating the suprathermal fluxes. A profile of plasma-line frequency versus altitude found by fitting a second-order polynomial to the observations has been used to calculate the expected plasma-line intensities. The agreement with the measurements is overall very good, both in the values of plasma-line intensities reached and the height distribution of the enhancements. The measured enhancements are sometimes confined to a slightly narrower height interval than the predictions; this may be due to fine structure in the suprathermal electron flux which is not well represented by the resolution of the calculations in Figure 7. Also, the highest intensities observed in each case are not quite reproduced by the model calculations. In

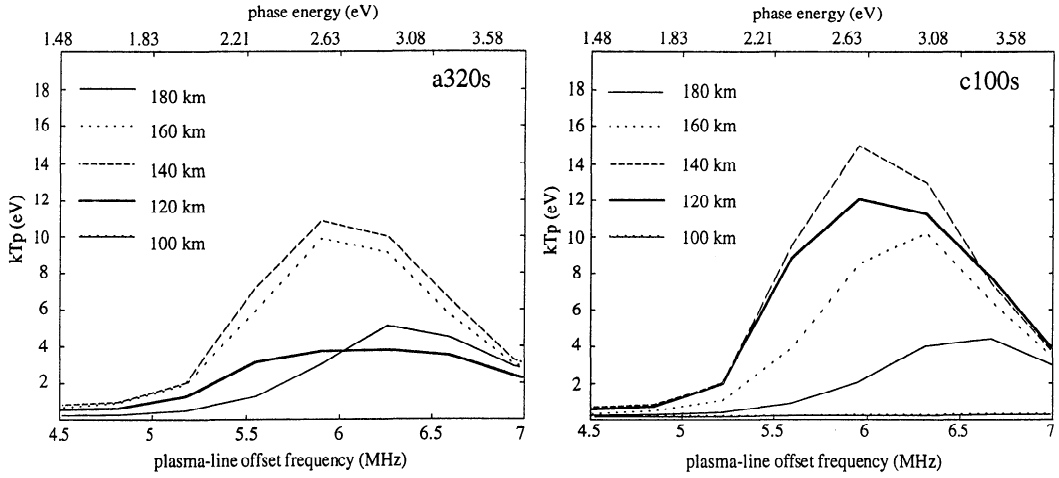

Figure 9. Plasma line intensities calculated using the flux-energy spectra in Figure 7 and (7) (see text for further details). The frequency scale assumes backscatter measurements with the EISCAT UHF radar, i.e., $f_{pl} = (E_\phi K^2 / 2m_e\pi^2)^{0.5}$, where K is 39 m^{-1}.

Table 1. Temperatures and Densities Used in the Calculations in Figures 8 and 9

Altitude	n_n ,m^{-3}	T_n, K	a320s			c110s		
			T_e, K	n_s,m^{-3}	max kT_p,eV	T_e,K	n_s ,m^{-3}	max kT_p,eV
100	7×10^{18}	200	200	1×10^{6}	0.02	200	2.10^{8}	0.3
120	3×10^{17}	397	397	2×10^{8}	4	397	1.10^{9}	12
140	5×10^{16}	695	695	3×10^{8}	11	900	8.10^{8}	15
160	2×10^{16}	883	1000	2×10^{8}	10	1500	7.10^{8}	10
180	7×10^{15}	1000	1600	2×10^{8}	5	2000	6.10^{8}	5

Here, n_n is the neutral number density, T_n the neutral temperature, T_e the electron temperature, n_s the total number density of the suprathermal electrons between 0.3 eV and 35 keV, and max kT_p the highest plasma-line intensity predicted by the calculations at each height.

the case of a320 s, 3 times higher suprathermal electron fluxes would be needed, and in the case of c 100 s, 10 times higher to produce the highest plasma-line intensities observed. It seems likely that, with 10 s time resolution, we do not fully resolve the peak intensity of the precipitation. The primary flux, and as a consequence, the suprathermal fluxes could be substantially higher for a shorter time. Very short duration (2-3 s) intervals of very intense fluxes (about 4 times our maximum energy flux in event c, 20 times our flux in event a) have indeed been suggested by other EISCAT observations in similar circumstanses [*Lanchester et al.*, 1994]. There is the additional possibility that fine structure in the N_2 absorption cross section on energy scales less than the resolution of the suprathermal flux model could cause higher peak plasma-line temperatures.

Interpretation: Plasma Turbulence

Mishin and Schlegel [1994] have proposed that strongly enhanced *E* region plasma lines might be a result of plasma turbulence. The scenario they propose is that long-wavelength Langmuir waves, driven directly by the high-energy primary particles, are converted by interaction with ion-acoustic waves to produce shorter wavelength Langmuir waves, appropriate to scatter the radar signal. Their scenario requires ion-acoustic waves enhanced 15-100 times above the thermal level, within a narrow layer corresponding to the narrow range of altitudes where the plasma lines are enhanced. In order for such a level of ion-acoustic waves to be achieved, there must be a field-aligned current and electron temperatures exceeding 4400 K. Plasma-line temperatures of about 1 eV are then predicted for phase energies less than ~1.6 eV, rising sharply to 5-10 eV for phase energies 1.9-2.5 eV. Also, according to this proposal the plasma-line intensities must continue to increase with phase energy (approximately as $E\phi^2$), i.e., with increasing wavelength of the Langmuir waves scattering the plasma line. This last feature would be expected for any mechanism depending on plasma turbulence, since an increase of energy toward longer scale sizes is an inherent feature of turbulence.

Our observations show this explanation cannot apply in the events shown here. First, we clearly see that the plasma-line intensities first increase with phase energy but then decrease again at phase energies above 3 eV (f > 6.5 MHz). Second, the electron temperatures associated

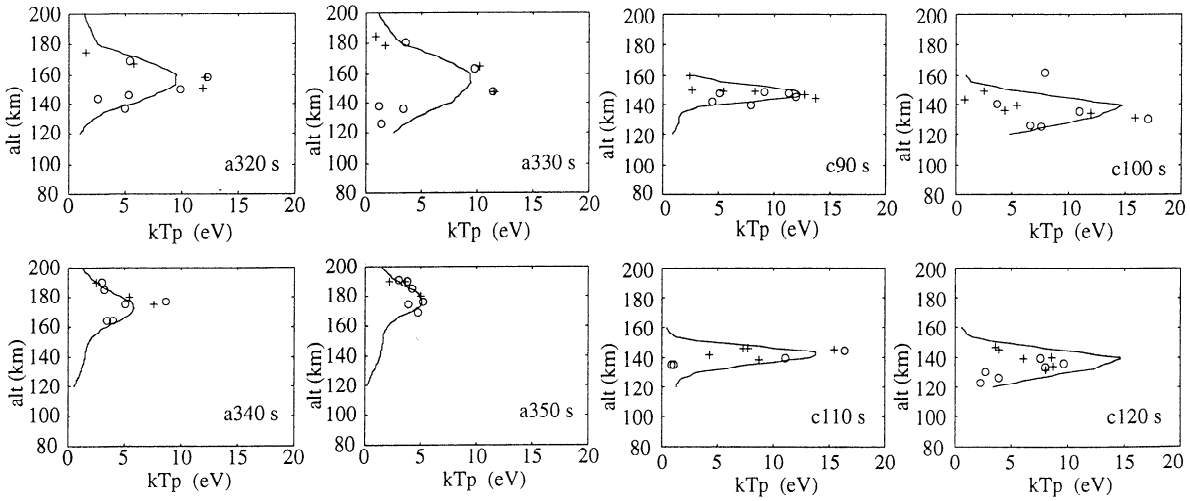

Figure 10. Comparison between measured plasma line temperatures (plus signs up-shifted, circles, down-shifted) and those calculated using the suprathermal electron fluxes in Figure 7 and (7).

with the most intense observed plasma lines are not particularly high, always less than 2500 K and usually less than 1000 K. For example, in event c, 90-120 s, the plasma lines are extremely strong and the electron density at the altitude of the plasma lines changes very little over a period of 40 s. The temperatures can be reliably determined from the plasma-line frequency in these circumstances and are less than 1000 K at the heights where the plasma lines are most intense. Since we measure the electron temperature using the plasma-line signal, we can be in no doubt that it is the temperature in the same volume of plasma where the plasma line is excited. Third, the enhanced ion-acoustic fluctuations required in this scenario would cause a similarly enhanced power in the incoherent scatter ion line, P_{ri}. The profiles of f_p' shown in Figures 2 and 3 are directly proportional to $(r^2 P_{ri})^{1/2}$. The proposed 15-100 times enhancement of ion-acoustic fluctuations would correspond to 4-10 times increase in the apparent value of f_p' in a thin layer at the altitude of the strongly enhanced plasma lines. There are quite clearly no such layers of enhanced ion-line power in the observed profiles. Last of all, since we can explain our observations by reasonable suprathermal electron fluxes, plasma turbulence is unnecessary.

Conclusions

Our observations confirm those of *Valladares et al.* [1988] in showing that strongly enhanced plasma lines can be observed during auroral precipitation. The enhancements we observed were even stronger than those reported by Valladares et al. up to 200 times the thermal level. We have further observed that the strongest enhancement is confined to a restricted frequency interval, 5.5-6.5 MHz, with only lower intensities occurring at both higher and lower frequencies. It seems that the enhancements cannot be explained by plasma turbulence, which would give ever increasing intensities at higher frequencies (for constant altitude and electron temperature) and strongly enhanced ion-line signals from the same altitudes, which we do not observe. We find, however, that the high intensities can be explained by reasonable suprathermal electron fluxes. The high intensities in a restricted frequency interval result from the minimum in suprathermal electron fluxes between 2 and 3 eV, which results from energy absorption into the vibrational levels of N_2. This, in turn, results in a minimum in the damping of Langmuir waves with corresponding phase energies. The frequent restriction of the plasma-line enhancement to a narrow altitude interval is explained by the sharp gradient in plasma frequency with altitude.

At the slightly higher frequency of the Sondrestrom radar, used by Valladares et al., these phase energies correspond to slightly higher frequency plasma lines. Valladares reported only weak plasma lines at 6.6 MHz and below, kT_p up to 3 eV at 7.0 MHz and up to 9 eV at 7.4 MHz. Frequencies 6.6, 7.0, and 7.4 MHz for the Sondrestrom k vector correspond to phase energies 1.7, 1.9, and 2.1 eV, respectively. Referring to Figure 9, it can be seen that this is exactly the phase energy range where we predict that the plasma-line enhancement starts to appear, i.e., Figure 9 shows kT_p <1eV at phase energy 1.7 eV, up to 2 eV at phase energy 1.9 eV and up to 5 eV at phase energy 2.1 eV.

The extremely high plasma-line intensities make the signal much easier to observe under just those conditions which may be most interesting, i.e. intense particle precipitation. This considerably improves the possibility to develop the use of plasma lines for studying suprathermal fluxes, high-time resolution temperature changes and possibly even field-aligned currents during auroral precipitation.

Acknowledgments. The EISCAT Scientific Association is supported by the Centre National de la Recherche Scientifique of France, Suomen Akatemia of Finland, Max Planck Gesellschaft of Germany, Norges Almenvitenskaplige Forskningsråd of Norway, Naturvetenskapliga Forskningsrådet of Sweden and the Science and Engineering Research Council of the United Kingdom. We thank E. Mishin for lively discussions and W. Kofman for his careful comments on the manuscript. The work of S.K. and H.N. is supported by the Naturvetenskapliga Forskningsrådet of Sweden.

The Editor thanks two referees for their assistance in evaluating this paper.

References

Bjørnå, N., and S. Kirkwood, Observations of natural plasma lines in the *E* region and lower *F* region with the EISCAT UHF radar, *Ann. Geophys., 4,* 137-144, 1986.

Cicerone, R.J., Photoelectrons in the ionosphere: Radar measurements and theoretical computations, *Rev. Geophys., 12,* 259-271, 1974.

Fredriksen, Å., N. Bjørnå, and T.L.Hansen, The first EISCAT two-radar plasma-line experiment, *J. Geophys. Res., 94,* 2727-2731, 1989.

Hagfors, T., and M. Lehtinen, Electron temperature derived from incoherent-scatter observations of the plasma-line frequency, *J. Geophys. Res., 86,* 119-124, 1981.

Hedin, A..E., Extension of the MSIS thermosphere model into the middle and lower atmosphere, *J. Geophys. Res., 96,* 1159-1172, 1991.

Kirkwood, S., SPECTRUM - A computer algorithm to derive the flux-energy spectrum of precipitating particles from EISCAT electron density profiles, *IRF Tech. Rep. 034,* Swedish Inst. of Space Phys., Kiruna, 1988.

Kirkwood, S., and N. Bjørnå, Electron temperatures determined by tristatic plasma-line observations with the EISCAT UHF incoherent scatter radar, *Geophys. Res. Lett., 19,* 661-664, 1992.

Kirkwood,S., and L. Eliasson, Energetic particle precipitation in the substorm growth phase measured by EISCAT and Viking, *J. Geophys. Res., 95,* 6025-6073, 1990

Kirkwood, S., P.N. Collis, and W. Schmidt, Calibration of electron densities for the EISCAT UHF radar, *J. Atmos. Terr. Phys., 48,* 773-775, 1986.

Kofman, W., G. and Lejeune, Determination of low-energy photo-electron distribution from plasma-line measurements at Saint Santin, *Planet. Space Sci., 28,* 661-673, 1980.

Kofman, W., and V. Wickwar, Plasma-line measurements at Chatanika with high-speed correlator and filter bank, *J. Geophys. Res., 85,* 2998-3012, 1980

Kofman,W., G. Lejeune, T. Hagfors, and P. Bauer, Electron temperature measurements by the plasma line technique at the

French incoherent scatter radar facilities, *J. Geophys. Res., 86*, 6795-6801, 1981.

Kofman, W., J.-P. St.-Maurice, and A.P. van Eyken, Heat flow effect on the plasma-line frequency, *J. Geophys. Res., 98*, 6079-6085, 1993.

Lanchester, B.S., J.P. Palmer, M.H. Rees, D. Lummerzheim, K.Kaila, and T. Turunen, Energy flux and characteristic energy of an elemental auroral structure, *Geophys. Res. Lett., 21*, 2781-2792, 1994.

Lilensten, J., D. Fontaine, W. Kofman, L. Eliasson, C. Lathuillere, and E.S. Oran, Electron energy budget in the high-latitude ionosphere during Viking/ EISCAT coordinated measurements, *J. Geophys. Res., 95*, 6081-6092, 1990.

Lummerzheim, D, and J. Lilensten, Electron transport and energy degradation in the ionosphere: evaluation of the numerical solution, comparison with laboratory experiments, auroral observations, *Ann. Geophys.*, in press, 1995.

Mishin, E, and T. Hagfors, On heat-flow contrrbution to plasma line frequency in the *F* region, *J. Geophys. Res., 99*, 6537-6539, 1994.

Mishin, E.V., and K. Schlegel, On incoherent-scatter plasma lines in aurora, *J. Geophys. Res., 99*, 11391-11399, 1994.

Newman, A., and E. Oran, The effects of electron-neutral collisions on the intensity of plasma lines, *J. Geophys. Res., 86*, 4790-4794, 1981.

Nicolet, M., The collision frequency of electrons in the ionosphere, *J. Atmos. Terr. Phys., 3*, 200-220, 1953.

Nilsson, H., S. Kirkwood, and N. Bjørnå, Bistatic measurements of incoherent-scatter plasma lines, *J. Atmos. Terr. Phys.*, in press, 1995.

Oran, E.S., V. Wickwar, W. Kofman, and A.L. Newman, Auroral plasma lines: A first comparison of theory and experiment, *J. Geophys. Res., 86*, 199-205, 1981.

Sharp, W.E., and P.B. Hays, Low-energy auroral electrons, *J. Geophys. Res., 79*, 4319-4321, 1974.

Valladares, C.E., M.C. Kelley, and J.F. Vickrey, Plasma line observations in the auroral oval, *J. Geophys. Res., 93*, 1997-2003, 1988.

Wickwar, V.B., Plasma lines in the auroral *E* layer, *J. Geophys. Res., 83*, 5186-5190, 1978.

Yngvesson, K.O., and F.W. Perkins, Radar Thomson scatter studies of photoelectrons in the ionosphere and Landau damping, *J. Geophys. Res., 73*, 97-110, 1968.

M. Galand, and J. Lilensten, CEPHAG-ENSIEG, BP 46, 38402 St. Martin d'Heres Cedex, France.

S. Kirkwood and H. Nilsson, Swedish Institute of Space Physics, Box 812, S-981 28 Kiruna, Sweden. (e-mail: sheila@irf.se; hane@irf.se.)

(Received September 19, 1994; revised January 13, 1995; accepted February 22, 1995.)